Numerical Investigation on Flow Separation Control of Low Reynolds Number Sinusoidal Aerofoils

I. H. Ibrahim[1]
University of Glasgow, Singapore

J. Joy[2] and T. H. New[2,*]
Nanyang Technological University, Singapore

The paper presents a computational analysis of the characteristics of a NACA 63_4-021 aerofoil incorporated with sinusoidal leading-edge protuberances at Re = 14,000. The protuberances are characterized by an amplitude and wavelength of 12% and 50% of the aerofoil chord length respectively. An unsteady Reynolds Average Navier Stokes (RANS) analysis of the full-span aerofoils was carried out using Transition SST (Shear Stress Transport) turbulence model across five different angles-of-attack (AOA). Comparisons with previous experimental results reported good qualitative agreements in terms of flow separation when the aerofoils are pitched at higher AOAs. Results presented here comprised of near-wall flow visualizations of the flow separation bubble at the peaks and troughs of the protuberances. Additionally, results indicate that the aerofoil with leading-edge protuberances displayed distinctive wall shear streamline and iso-contour characteristics at different span-wise positions. This implies that even at a low Reynolds number, implementations of these leading-edge protuberances could have positive or adverse effects on flow separation.

I. Keywords

NACA 63_4-021 aerofoil, Leading-edge protuberances, Low Reynolds, Flow separation bubble, Wall shear streamlines.

II. Introduction

ACHIEVING optimal flow control standards remains one of the holy grails in the study of aerodynamics. Some of the novel forms of flow control include the utilization of plasma actuators[1] which harness the bombardments of neutral particles in air that results in jets which could affect the characteristic mean flow on an aerodynamic surface. More recently though, there has been a resurgence in the study of passive flow control methods, particularly in the biomimetic form.

The investigation of aerofoils with leading-edge protuberances is an example of biomimetic flow control method. Studies into its operation at low Reynolds numbers have spurred particular interests recently, due to their intriguing design characteristics and effects on flow separation behavior and vortex generation[2,3]. This research area draws its inspirations from the morphology of humpback whales which possess exceptional maneuvering and turning ability at higher velocities, especially when they are approaching their preys. It has been determined by earlier studies that the swiftness in the motion of a humpback whale is partially affected by the presence of pectoral flippers with leading-edge protuberances[3].

A detailed aerodynamic performance analysis of flippers with leading-edge protuberances was experimentally conducted by Miklosovic et al.[4] at Re = 5×10^5. The flippers were based on the symmetrical NACA 0020 aerofoil. The reported results showed a significant increase in the maximum lift of aerofoil structures with leading-edge protuberances by 6%, as compared to the ones with the unmodified aerofoil structure. In addition, the stall angle increased considerably by about 40% in the presence of leading-edge protuberances.

Performance analysis of NACA 63_4-021 aerofoils have also been conducted successfully in previous investigations by Johari et al.[5] and Zhang et al.[6]. In particular, there have been experiments[5] conducted on a modified NACA 63_4-021 with different protuberance wave amplitudes and wavelengths. The results indicate

[1]Assistant Professor, Assistant Professor in Aeronautical Engineering (Aerospace Sciences), University of Glasgow, imran.ibrahim@glasgow.ac.uk, AIAA Member
[2]M.Sc. Student, School of Mechanical and Aerospace Engineering, m130147@e.ntu.edu.sg.
[*]Assistant Professor, School of Mechanical and Aerospace Engineering, dthnew@ntu.edu.sg, AIAA Member. Corresponding author, dthnew@ntu.edu.sg

that there is a significant reduction in maximum lift coefficient in the presence of leading-edge protuberances in the pre-stall region. However, the post-stall lift coefficient is enhanced as much as by 50% and the drag coefficient is reduced considerably in the post-stall region.

Numerical simulations of the NACA 63_4-021 aerofoils have been also conducted to shed light on the overall flow structure of the modified aerodynamic surface. A recent numerical investigation of modified aerofoils reported by Cai[3] presents conclusions at Re = 1.83 x 10^5 similar to those for the past experimental data. The

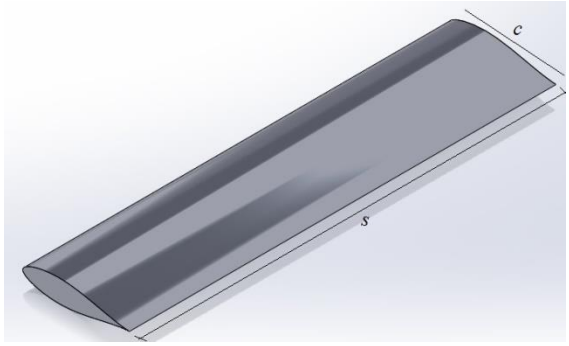

a) Isometric view of the baseline NACA 63_4-021 aerofoil.

b) Top view of the baseline aerofoil, with dimensions of the span and chord.

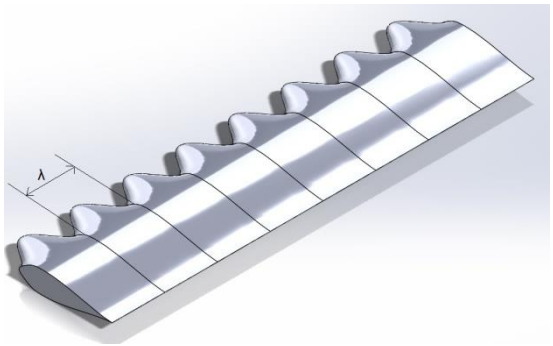

c) Isometric view of the 8L modified NACA 63_4-021 aerofoil.

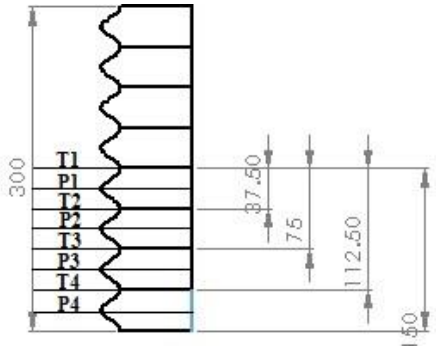

d) Top view of the 8L modified NACA 63_4-021 aerofoil, with dimensions of the span and protuberance wavelength.

Figure 1. Computer Aided Design profiles of the aerofoil (measurements in mm).

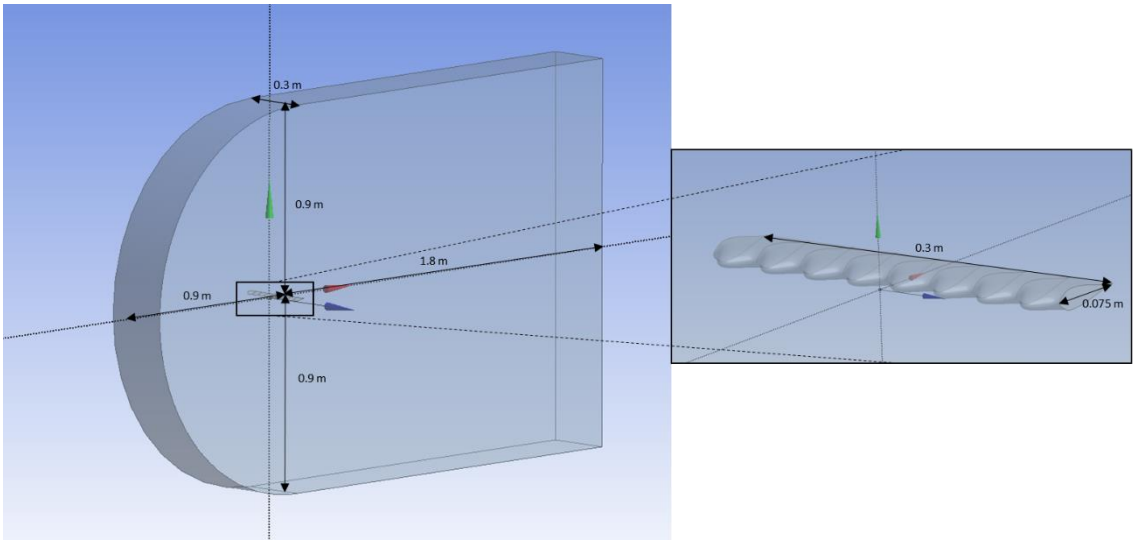

Figure 2. Simulation domain used in the analysis

numerical investigation further validates that aerofoils with leading-edge protuberances are able to increase lift coefficient and decreased drag coefficient at the post-stall region.

In this paper, a numerical investigation was conducted on a baseline and a modified NACA 63_4-021 aerofoil profiles (shown in Figure 1) at Re = 14,000. Previous research and observations had indicated that the pectoral flipper match significantly with that of a NACA 63_4-021 aerofoil profile[5]. In addition, the leading-edge protuberances along the span-wise direction were sinusoidal by nature. The two-equation Shear Stress Transport (SST) turbulence model was implemented in the current investigation. The current work aims to further investigate the studies conducted by Wei et al.[2] by looking into the wall shear streamlines, vector plots as well as iso-surface contours of shear at the vicinity of the aerofoil. The present investigations also extend the study conducted by Joy et al.[7] by utilizing a structured hexahedral grid for the simulations. As the applicability of low Reynolds number aerodynamics (i.e. Re = 10^4 to 10^6) encompasses High Altitude Low Endurance (HALE) Reconnaissance airplanes, Micro Aerial Vehicles as well as insects and birds flight[6], the range of flow control authority imposed on the aerofoil by the protuberances would be further verified.

III. Computational Study

A modified aerofoil with leading-edge protuberances was designed and presented in Figure 1. The modified aerofoil was designed with a characteristic mean chord, c = 75mm and span, s = 300mm. The wavelength and amplitude dimensions of leading-edge protuberances for this modified aerofoil are $\lambda = 0.5c$ and $A = 0.12c$. The velocity streamlines, aerofoil lift and the span direction fits in x, y and z-coordinates of the designed model. The origin of the aerofoil is defined along the leading-edge of the mean chord. The dimensions of the computational domain are shown in Figure 2. As the goal of the present study is to get an understanding of the flow features on the surfaces of the aerofoil, a symmetry boundary condition is prescribed at the sides of the domain, permitting the domain width to be has its similar to the span length of the aerofoil.

The simulations were conducted on Ansys Fluent[8] and the setup employed a structured, hexahedral grid that fitted the complex three-dimensional geometry of the model. The mesh, shown in Figure 3, was generated using edge sizing, defining number of edge points and the input of inflation layers gave overall y+ less than 5. These inflation zones are expected to produce better boundary layer resolution close to the aerofoil surface. The 3D simulation consists of a total number of elements approximated 1 x 10^6.

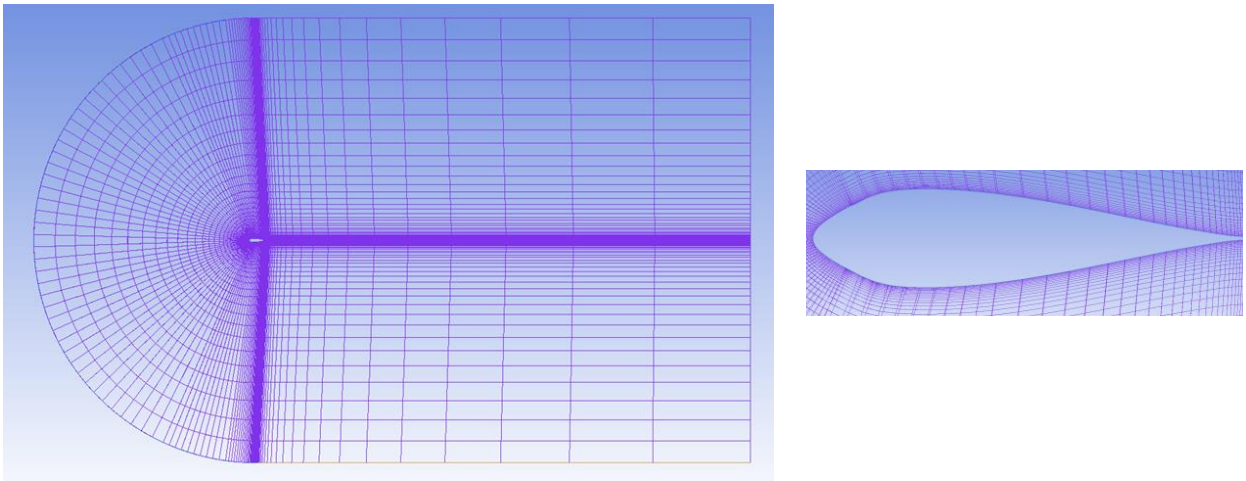

a) Side view of the mesh Grid on NACA 63_4-021. **b) A closer look on Grid structure of 8L hydrofoil.**

Figure 3. The discretized simulation domain.

The simulations were carried out using Reynolds Averaged Navier-Stokes (RANS) with the Transition SST (Shear Stress Transport) model implemented as turbulence. Similar to that had been noted by Rostamzadeh et al.[9], the turbulence model had been selected for the expected production of transitional flow features such as Laminar Separating Bubbles (LSB) to be formed near the vicinity of the aerofoils. The defining parameter in both steady and transient state computation is the inlet velocity of 0.19 m/s corresponding to Re = 14,000 and a turbulence intensity of 1.1%. The time steps defined is 0.001 for all computations and each simulation is run to achieve 20 seconds of flow-field at convergence criteria of 10^{-5}.

IV. Results

A. Laminar Separation Bubble

Comparisons of the results with earlier experiments[2] were conducted on both baseline and modified aerofoils at an AOA of $\alpha = 20°$. It should be mentioned that the particle-image velocimetry experiments conducted in in Wei et al.[2] followed procedures similar to Lim et al.[10], New and Tsovolos[11,12] and New et al.[13]. It is known that the presence of significant flow separation bubbles is usually an indication of poor performance for an aerodynamic surface. The streamlines were plotted at the mid-span region of the baseline aerofoil. For the modified aerofoils, the streamlines were plotted at the trough and peak sections of the aerofoil. The simulation results are generally in good agreement with experimental findings except for the separation bubble located at the peak location when the modified aerofoil is at $\alpha = 20°$. The dominant recirculation region is captured for the baseline aerofoil in both the experiment and simulation results. At the trough locations, both the experiment and simulation results show that the large recirculation region has shifted slightly forward of the trailing-edge. A smaller recirculation region can also be seen at the trailing-edge of the aerofoil. At the peak locations however, the experimental result seems to indicate that the circulation region located at the mid-chord section of the aerofoil is developing and will not sustain its strength and form. The results for both experiment and simulation indicate a large bubble forming close to the trailing-edge of the aerofoil. At the trough location of the modified aerofoil, two recirculation regions are recorded for both the experiment and simulation.

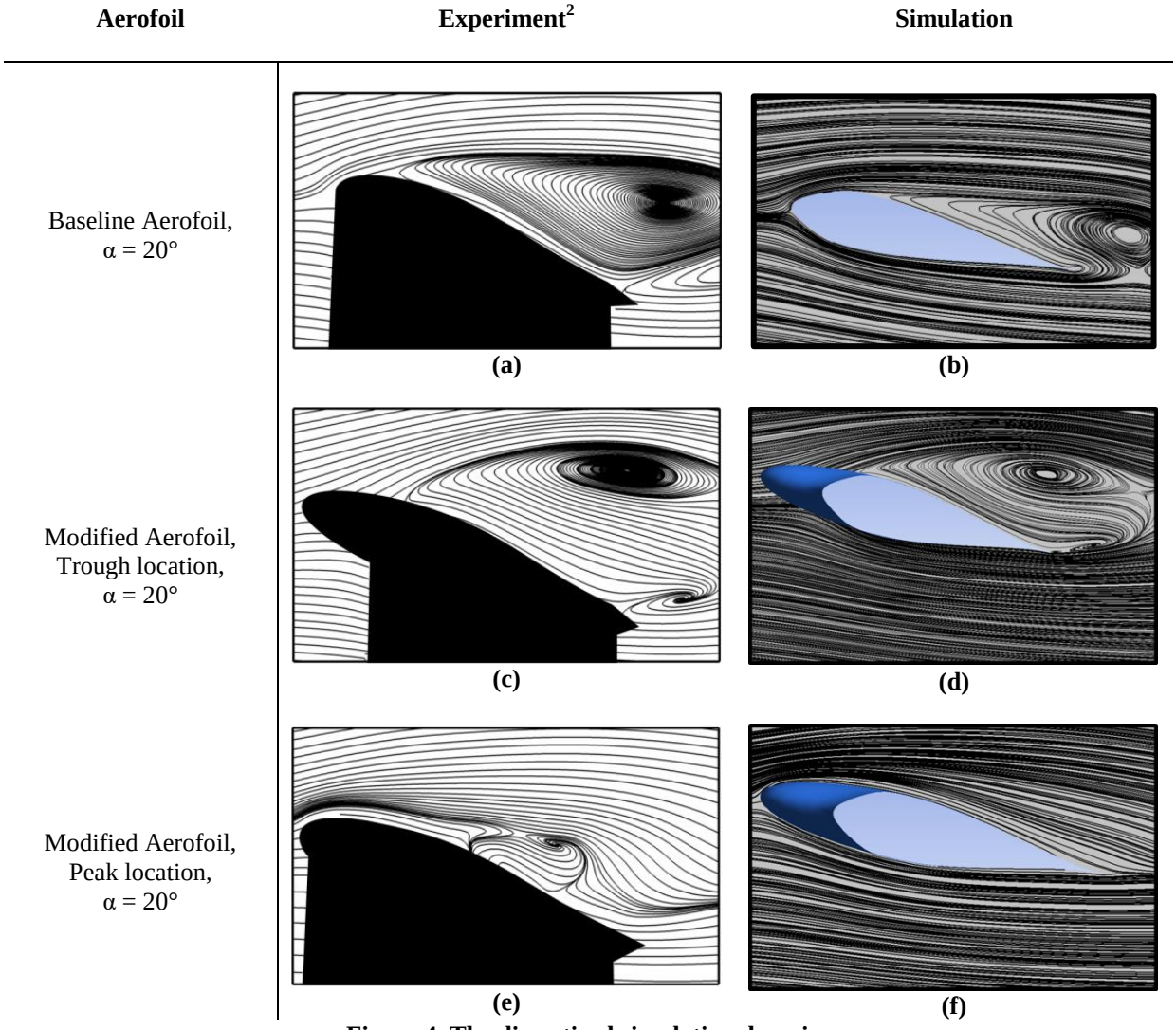

Figure 4. The discretized simulation domain.

B. Wall Shear Streamlines

Wall shear streamlines are plotted in both forward and backward directions relative to the flow direction as indicated from bottom to top in Figure 5. The streamlines are plotted on the surfaces of the baseline aerofoil to indicate possible locations of flow separations. The aerofoil is pitched at 0°, 10°, 15° and 20°. Vectors are not plotted in this figure, but it can be postulated that the misalignment of the streamlines are due to the forward and backward stream directions. This will be clearly shown in a later figure. The region (red line) where the both streamline directions meet is indicates flow separation. As the aerofoil is pitched higher, the red line moves closer towards the leading edge of the aerofoil.

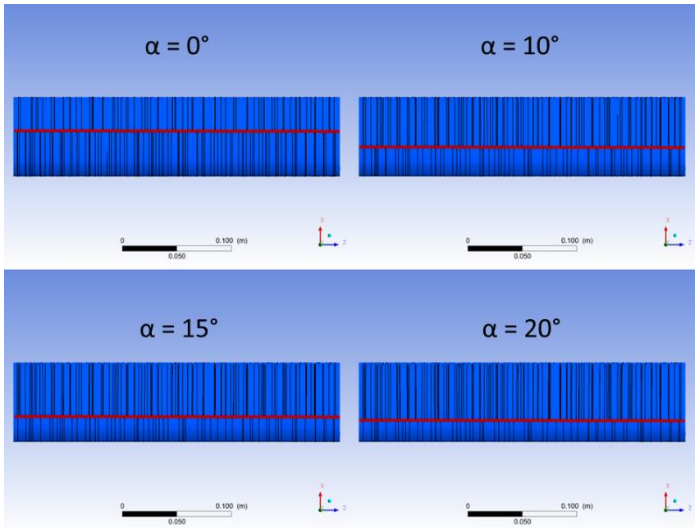

Figure 5. Wall shear streamlines of the baseline aerofoil at 0°, 10°, 15° and 20° AOA.

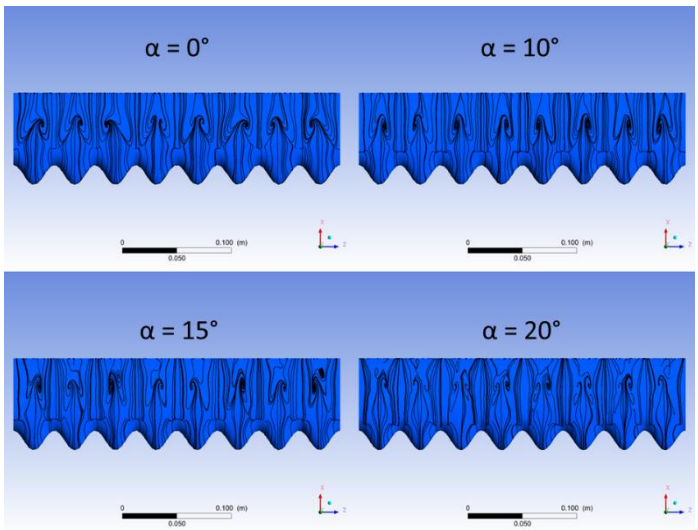

Figure 6. Wall shear streamlines of the modified aerofoil at 0°, 10°, 15° and 20° AOA.

Wall shear streamlines on the modified aerofoil show significant span-wise variation throughout the suction side as seen in Figure 6. A key feature of the streamlines on the modified aerofoil is the presence of regular recirculation zones about 60% downstream along the chord-wise direction of the aerofoil. The recirculation seems to be formed via streamlines enjoined from the leading and trailing edges of the aerofoil. Greater irregularities in the recirculation can also be seen as the aerofoil is pitched higher, with the results at 20° suggesting a splitting of the recirculation into two portions. Collating with studies mentioned earlier, these recirculation regions are associated with the streamwise vortices produced by the leading-edge protuberances.

C. Wall Shear Iso-Surface

Figure 7 shows regions of negative wall shear stress relative to the mean direction of the flow (x-axis). The regions in gray correlate with the areas where the wall shear stress are in the negative direction as shown in Figure 5 and provides a scale at which the separated flow is relative to the size of the aerofoil. The results indicate that this region of separated flow increase with increasing pitch angles. Also, there seems to be an increasing flow reattachment region at the trailing edge of the aerofoil. This is initially seen at $\alpha = 10°$ but becomes more predominant at $\alpha = 15°$ and 20°.

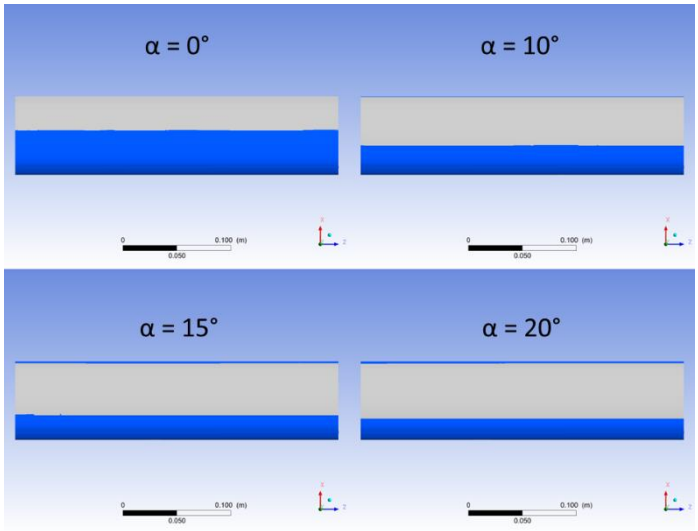

Figure 7. Negative wall shear (x-direction) for the baseline aerofoil at different angles of attack.

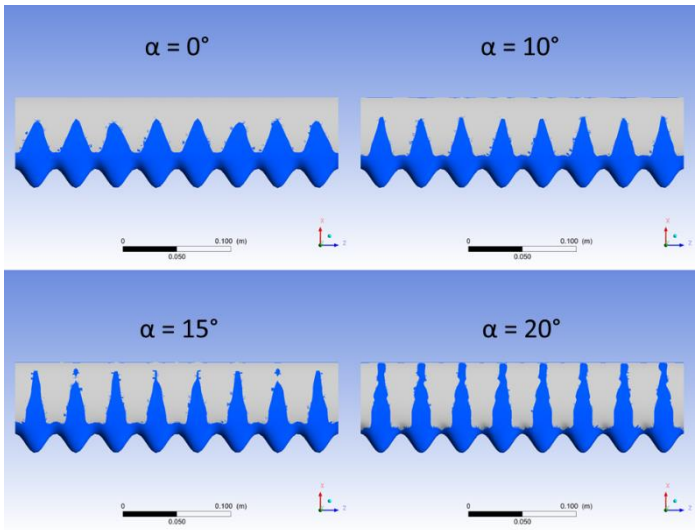

Figure 8. Negative wall shear (x-direction) for the modified aerofoil at different angles of attack.

As expected, the regions indicating negative wall shear in the x-direction for the modified aerofoil indicates spanwise dissimilarity throughout the suction side of the aerofoil. Two main observations can be seen here. Firstly, the flow tends to be dominated by an increasing separated region immediately downstream of the trough of the tubercles. This can be deduced by the increase in gray regions observed as the aerofoil is pitched at higher AOA. Secondly, with the increasing area of separation seen downstream of the troughs, a similarly increasing region of flow attachment can be seen downstream of the peak. Again this is deduced by the blue regions. The presence of the recirculation regions seen from the wall shear streamlines in Figure 6 suggest an inflicted re-energization of the boundary layer at the vicinity, resulting in the improved flow attachment characteristics. In particular, this reinforces the notion that the streamwise vortices are able to draw free-stream fluid towards the suction side of the modified aerofoil and energize the boundary layer.

D. Wall Shear Vector and Streamlines

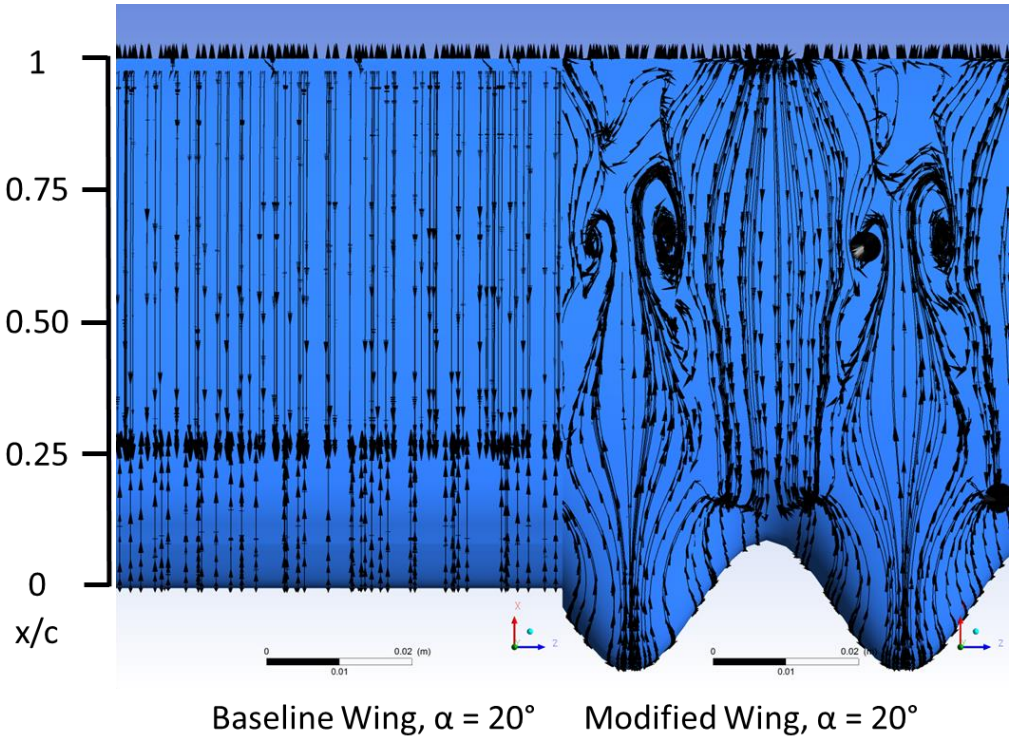

Figure 9. Streamlines and velocity vector plots for the baseline and modified aerofoil pitched at 20°

Combined vector and streamline plots are shown in Figure 9. Typically speaking, the forward-moving streamlines emanate from the aerofoil leading-edge and vice versa for the backward-moving streamlines. For the baseline aerofoil, the streamlines terminate at separation points located uniformly along the streamwise direction of the aerofoil, as expected. For the modified aerofoil however, there seems to be a convergence of the forward-moving streamlines that emanate primarily from the peaks of the tubercles. Similar to that observed by Rostamzadeh et al.[9], in the absence of any lateral strain in this region, streamlines which initiate near the peak of the tubercles initially converge at 0.1*c*, diverge at 0.25*c* before converging again at 0.5*c*. At 0.625*c*, the streamlines divide themselves into two regions, with each region recirculating in nature. The divergence at 0.25*c* consists of both the recirculating zones observed at 0.625*c*.

Moving further away from the tubercle peaks, streamlines initiating from these regions meander towards the area slightly downstream of the trough instead. Again, this feature concurs with the findings by Rostamzadeh et al.[9]. The curvatures from the streamlines imply that the pressure gradient is directed towards the trough region of the modified aerofoil. From the vector plots, it can be seen that the bulk of the flow originates from the backward-moving streamlines. These streamlines emanated from a part of the trailing-edge of the aerofoil which is directly downstream. Part of the trailing-edge streamlines emanation, however, shows contribution to the recirculation region which was initially formed by the forward moving streamlines.

V. Conclusions

A computational study on NACA 63_4-021(baseline) and modified aerofoils with sinusoidal leading-edge protuberances was performed at Re = 14,000 at different angles of attack. The presence of the protuberances has a profound effect in the wall shear streamlines associated with the surfaces of the modified aerofoil. The modification enhances the span-wise variation of the streamlines and is hypothesized to have a positive effect on flow separation mitigation, especially when the aerofoil is pitched at higher AOA. Results pertaining to the flow separation bubbles seen in simulation generally agree with the experimental results reported by Wei et. al[2]. The results indicate that even at very low Reynolds number, leading-edge protuberances may be used as effective passive flow control devices.

VI. Acknowledgments

The authors gratefully acknowledge the support provided for the study through a MINDEF Defense Innovative Research Project Research Grant, as well as the assistance provided by Wei Zhaoyu in the designing of the aerofoils with leading-edge protuberances used here.

VII. References

[1]Ibrahim, I., and Skote, M. "Effects of the scalar parameters in the Suzen-Huang model on plasma actuator characteristics," *International Journal of Numerical Methods for Heat & Fluid Flow* Vol. 23, No. 6, 2013, pp. 1076-1103.

[2]Wei, Z., New, T. H., and Cui, Y. D. "An experimental study on flow separation control of hydrofoils with leading-edge tubercles at low Reynolds number," *Ocean Engineering* Vol. 108, 2015, pp. 336-349.

[3]Cai, C., Zuo, Z., Liu, S., and Wu, Y. "Numerical investigations of hydrodynamic performance of hydrofoils with leading-edge protuberances," *Advances in Mechanical Engineering* Vol. 7, No. 7, 2015.

[4]Miklosovic, D. S., Murray, M. M., Howle, L. E., and Fish, F. E. "Leading-edge tubercles delay stall on humpback whale (Megaptera novaeangliae) flippers," *Physics of Fluids* Vol. 16, No. 5, 2004, pp. L39-L42.

[5]Johari, H., Henoch, C., Custodio, D., and Levshin, A. "Effects of leading-edge protuberances on airfoil performance," *AIAA Journal* Vol. 45, No. 11, 2007, pp. 2634-2642.

[6]Zhang, R.-K., and Wu, J.-Z. "Aerodynamic characteristics of wind turbine blades with a sinusoidal leading edge," *Wind Energy* Vol. 15, 2012, pp. 407-424.

[7]Joy, J., New, T. H., and Ibrahim, I. H. "A Computational Study on Flow Separation Control of Humpback Whale Inspired Sinusoidal Hydrofoils," *World Academy of Science, Engineering and Technology, International Journal of Mechanical, Aerospace, Industrial, Mechatronic and Manufacturing Engineering* Vol. 10, No. 2, 2016, pp. 344-349.

[8]"ANSYS® Academic Research, Release 16.2." 2015.

[9]Rostamzadeh, N., Hansen, K. L., Kelso, R. M., and Dally, B. B. "The formation mechanism and impact of streamwise vortices on NACA 0021 airfoil's performance with undulating leading edge modification," *Physics of Fluids* Vol. 26, No. 10, 2014, pp. 1-22.

[10]Lim, T. T., New, T. H., and Luo, S. C. "Scaling of Trajectories of Elliptic Jets in Crossflow," *AIAA Journal* Vol. 44, No. 12, 2006, pp. 3157-3160.

[11]New, T. H., and Tsovolos, D. "Influence of nozzle sharpness on the flow fields of V-notched nozzle jets," *Physics of Fluids* Vol. 21, No. 8, 2009, p. 084107.

[12]New, T. H., and Tsovolos, D. "On the vortical structures and behaviour of inclined elliptic jets," *European Journal of Mechanics - B/Fluids* Vol. 30, No. 4, 2011, pp. 437-450.

[13]New, T. H., Chan, Y. X., Koh, G. C., Hoang, M. C., and Shi, S. "Effects of Corrugated Aerofoil Surface Features on Flow-Separation Control," *AIAA Journal* Vol. 52, No. 1, 2014, pp. 206-211.